Working document

March 3, 2020

General idea: How can the terrestrial plant literature on seed bank be applied to phytoplankton coexistence?

Introduction

The high biodiversity of plant communities has long been a subject of both experimental and theoretical ecologists. Both terrestrial plants and phytoplanktonic communities can present hundreds of species which seem to consume the same resources. First theoreticians have proposed that environmental fluctuations [ref] could sustain such coexistence but further research have proved that this could not actually explain the observed richness of species communities [ref]. Other mechanisms such as niche differentiation or neutral theory have completed environmental variation and stochasticity to solve this question [ref]. The role of demography and life history traits also proves important [ref].

Analyses of coexistence in terrestrial plant communities often take into account several life stages [refs]. Considering at least two stages, seeds/juveniles and adults, different models have uncovered mechanisms that might explain long-term coexistence. Examples of such mechanisms are the bet-hedging strategy, the storage effect and the Janzen-Connell effect. Bet-hedging is a long-term strategy relying on the creation of seeds which can remain dormant for a long period of time (over a year, often much longer). Dormant seeds can tolerate harsher years during which adults cannot maintain, but they also reduce part of the population that could germinate from one year to another (in case of an annual plant). The storage effect has first been defined by the presence of a long-lived life stage and temporal variation in recruitment from this long-lived life stage that helps escape interspecific competition (Chesson 1986, Cáceres, 1997). This has been later generalized as a negative correlation between the effect of the environment and the effect of competition (Ellner et al. 2016). In good enviromental conditions, competition from other individuals is stronger as seeds might germinate at the same time. Finally, models and experiments suggest that adults can have a negative effect on seed survival, through the Janzen-Connell effect (Comita et al. 2014).

Even though different coexistence mechanisms have been unveiled through the use of several life stages and a focus on the youngest stage (seeds) for terrestrial plants, aquatic plants, and more specifically phytoplanktonic algae, have not been modeled with the same precision. Although theoreticians have proposed for a long time that the blooms may initiate after the resuspension and germination of seeds (Patrick 1948, Marcus and Boero 1998), it is unusal to see an explicit model of such process [[Note: not necessarily theoreticians, but they have done small review of the existence of spores and the possible benthic-pelagic coupling.]]. The classical view behind phytoplankton dynamics is that bloom formation is mostly seasonal, due to the variation in light and temperature, assuming that there are always enough cells in the environment to duplicate. However, a recent review suggests that there might be more complexity behind phytoplanktonic seeds/cysts (Ellegaard & Ribeiro, 2018). Neglecting explicit modeling of this life stage can modify the understanding we have of the dynamics of the populations (Nguyen *et al.*, 2019).

Phytoplankton communities in coastal environments may benefit from seed banks even more than the oceanic communities, as the distance to the bottom is lower. Similarly to the seed bank approach, Smayda (2002) has

proposed the term "pelagic seed bank" to characterize the contribution of the ocean to coastal communities. This has been noticed for dinoflagellate especially [[ref Dinophysis, check what we have on diatoms]]. We can wonder, however, to which extent the seed banks can contribute to the biodiversity in the ocean, especially in the long term. Indeed, spores are able to germinate again after tens of years (McQuoid *et al.*, 2002; Ellegaard & Ribeiro, 2018) or even thousands of years (Sanyal *et al.*, 2018) of dormancy, which can play a huge role on biodiversity in both oceanic and coastal environments.

Here we build on the work by Shoemaker & Melbourne (2016); Wisnoski *et al.* (2019), and previous findings inPicoche & Barraquand (2019, 2020), to examine the effect on coexistence and feedbacks from the different compartments (ocean, coastal water column and bottom).

Methods

Model

The model developed by Shoemaker & Melbourne (2016); Wisnoski *et al.* (2019) builds on a two-step discrete-time model: the abundances of cells present in the coastal or oceanic waters first increase following Beverton-Holt dynamics. The Beverton-Holt (BH) formulation is classical for discrete-time models of terrestrial plants and includes both maximum growth rates and the effects of positive and negative interactions on said growth rates. In our models, the maximum achievable growth rate for one time step is dependant on both the species and the current temperature. During the same first step, the abundance of cells present at the bottom of the floor in coastal areas (hereafter called cysts) decreases due to both cyst mortality and the burial **consécutif** to sedimentation. During the second step, exchanges take place between the different compartments,

$$\begin{cases} N_{t+h,i,c/o} &= \frac{e^{r_i(T)} N_{t,i,c/o}}{1+\sum_j \alpha_{ij,c/o} N_{t,j,c/o}} \\ N_{t+h,i,b} &= N_{t,i,b}(1-m_i-\zeta_i) \end{cases} \tag{1}$$

with $r_i(T)$ was calibrated for this study (see SI for more information) and interactions are inferred from previous work on real data with a Multivariate AutoRegressive (MAR) model. The shift from MAR to BH- matrices of interactions is described in SI.

$$\begin{cases} N_{t+1,i,c} &= N_{t+h,i,c}(1-s_i-e)+\gamma_i N_{t+h,i,b}+eN_{t+h,i,o} \\ N_{t+1,i,o} &= N_{t+h,i,o}(1-s_i'-e)+eN_{t+h,i,c} \\ N_{t+1,i,b} &= N_{t+h,i,b}(1-\gamma_i)+s_i N_{t+h,i,c} \end{cases} \tag{2}$$

Parameters and state variables definitions are given in Table 1. Each compartment (ocean, coast, seed bank) contain 10^6 cells at the beginning of the simulation, which is run for 10000 time steps.

Param	Name	Value (unit)
$N_{t,i,c/o/b}$	Abundances of species i at time t in the coast (c) or ocean (o) water column, or in the benthos (b)	NA (Number of cells)
T	temperature	NA (K)
r_i(T)	growth rate of species i	NA
b_i	Normalization constant for the thermal decay rate	(K^3)
τ_0	Reference temperature	293 (K) / 20 (°C)
$a_r(\tau_0)$	Growth rate at reference temperature	$386(\frac{\text{kg}}{\text{kg}\times\text{year}})^1$
E_r	Activation energy	0.467 (eV)
k	Boltzmann's constant	$8.6173324.10^{-5}$(eV.K^{-1})
A	Niche area	15 [calibrated]
$f_i(T)$	Fraction of the maximum rate achieved for the i^{th} species	(NA)
$T_{\min}$	Minimum thermal optimum	Will be calibrated
$T_{\max}$	Maximum thermal optimum	Will be calibrated
T_i^{opt}	Optimal temperature for species i	Adapted from Picoche & Barraquand (2020)
$\alpha_{ij,c/o}$	interaction strength of species j on i	Adapted from Picoche & Barraquand (2020)
k_{c2o}	conversion coefficient from coastal to oceanic interactions	1.5 [arbitrary]
m_i	cyst mortality of species i	$\approx 10^{-4}/10^{-5}$(McQuoid *et al.*, 2002)
ζ_i	cyst burial	
s_i,s_i'	sinking rate of species i in a coastal environment	$0.3\beta(0.55, 1.25)$ (Passow, 1991)
e	exchange rate between ocean and coast	0.64 d^{-1} (Plus *et al.*, 2009)
γ_i	germination + resuspension rate of species i	[0.1,0.01,0.001] * [10^{-5},0.1] (abitrary)

Table 1: Definition of variable states and parameters

Optimal temperature Each species is defined by its own thermal optimum. However, the variability of this temperature is high, even within a single genus. A qualitative calibration of thermal optima based on the phenology of the groups we consider seems to be the more realistic approach.

Exchange rate This parameter depends on the estuary. In the Arcachon Bay, the exchange rate for each tide has been estimated around 64% (Plus *et al.*, 2009)[2].

Cyst mortality As previously mentioned, cyst loss is a composite of cyst mortality and inaccessibility. McQuoid *et al.* (2002) provides values of maximum depth at which cysts can still germinate for different species, leading to mortality values around $10^{-4}/10^{-5}$ (for more details on the approximation of mortality rate from maximum depth, see SI).

However, cyst burial might be a prevailing phenomenum in driving phytoplanktonic dynamics. Even when seeds can be resurrected, they are not accessible after being buried. This value needs to be calibrated in our model.

Sinking rate According to Passow (1991) (who measured sinking rates in real conditions), rates can vary between 1 and 30% for the same species (Chaetoceros spp.), with a mean value for two diatom species of 10 (Chaetoceros and Thalassiosira). Values are much for the others, around 1% for the others.

Sinking rate values around 10% are consistent with the loss rate values in Wiedmann *et al.* (2016).

We can arbitrarily fix a beta distribution with mean value close to the one observed in both papers (between 9 and 10), and maximum around 30%, that is $s \backsim \beta(0.55, 1.25) * 0.3$[3].

[1] As the final dimension of this variable is year-1, I don't think we have to convert to number of cells but I am still wondering about the usability of this parameter + we have to convert from year to day

[2] We need to have very good arguments to take into account only one tide per day.

[3] I do think this will need to be varied a lot

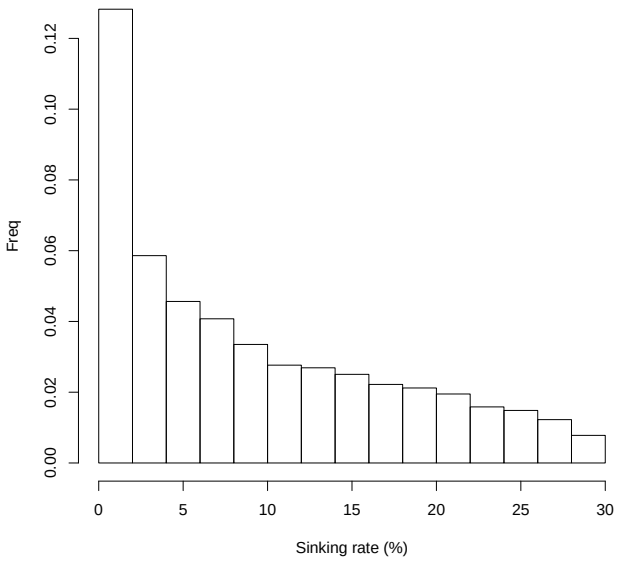

Figure 1: Possible distribution of sinking rates

Germination/resuspension Germination and resuspension might be difficult to differentiate, they are defined by the same parameters (γ = resuspension*germination). Even though we have no estimation of germination and resuspension rate, we can try several values.

Germination can be 1%, 0.1%, 0.01%. from McQuoid *et al.* (2002), we can assume that there is a temperature threshold for germination (but this cannot explain a lot of long-term dormancy) and the existence of such threshold is confirmed by the review by Agrawal (2009). Photoperiodicity does not seem to have a strong effect according to this review (but see Eilertsen *et al.* (1995)). We use a temperature threshold at 15°C.

Resuspension values vary from one publication to another: in Fransz & Verhagen (1985), resuspension rate of sediments is evaluated around 5.10^{-5} day^{-1} in winter and decreases in summer (there is a link between resuspension/sinking and light extinction coefficient). In Kowe *et al.* (1998), resuspension rate of diatoms is evaluated around $1.9.10^{-5}$ day^{-1}, with a maximum sinking rate of 0.085 day^{-1}. In Le Pape *et al.* (1999), resuspension rate of sediments and dead diatoms is 0.002 day^{-1}. In this paper, we will examine values between 10^{-5} (stratified water column) to 0.1 (highly mixed environment).

Calibration

Groups of species (Table 2), interaction matrices (Fig. 5) and realistic environmental conditions are taken from one of the sites (Auger) in a previous analysis based on field data (Picoche & Barraquand 2020), which shows the longest time-series for the most common groups of species.

Code	Taxa
CHA	*Chaetoceros*
DIT	*Ditylum*
GUI	*Guinardia*
LEP	*Leptocylindrus*
NIT	*Nitzschia+Hantzschia*
PLE	*Pleurosigma+Gyrosigma*
PRO	*Prorocentrum*
PRP	*Protoperidinium+Archaeperidinium+Peridinium*
PSE	*Pseudo-nitzschia*
SKE	*Skeletonema*
THP	*Thalassiosira+Porosira*

Table 2: Name and composition of the groups of species present in our reference site.

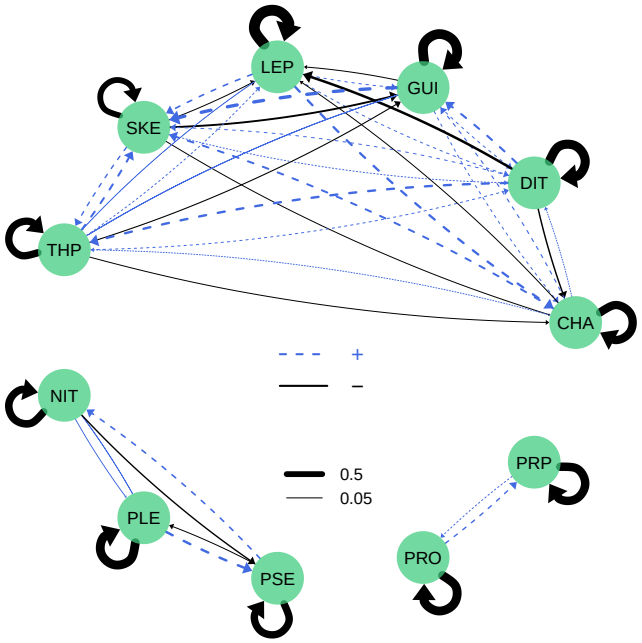

Figure 2: Description of the interaction networks in Auger

Growth rates and phenologies are used to calibrate the model.

Scenarios

In addition to sensibility analyses on parameters we cannot directly know (burial, sinking, resuspension, germination rates), scenarios can be proposed to study the effect of a seed bank on coexistence of species, by (1) removing such seed bank (by setting seed mortality to 1) and (2) removing the exchanges between the coast and the ocean (e=0). Final richness and average abundances are first diagnostics for such scenarios.

Results

Quadratic programming

Using quadratic programming as a way to tune parameters on the observed abundances leads to changes in parameter values. Some interactions can be multiplied by 80 after re-calibration (LEP/GUI) while most of the parameters

remain in the same domain.

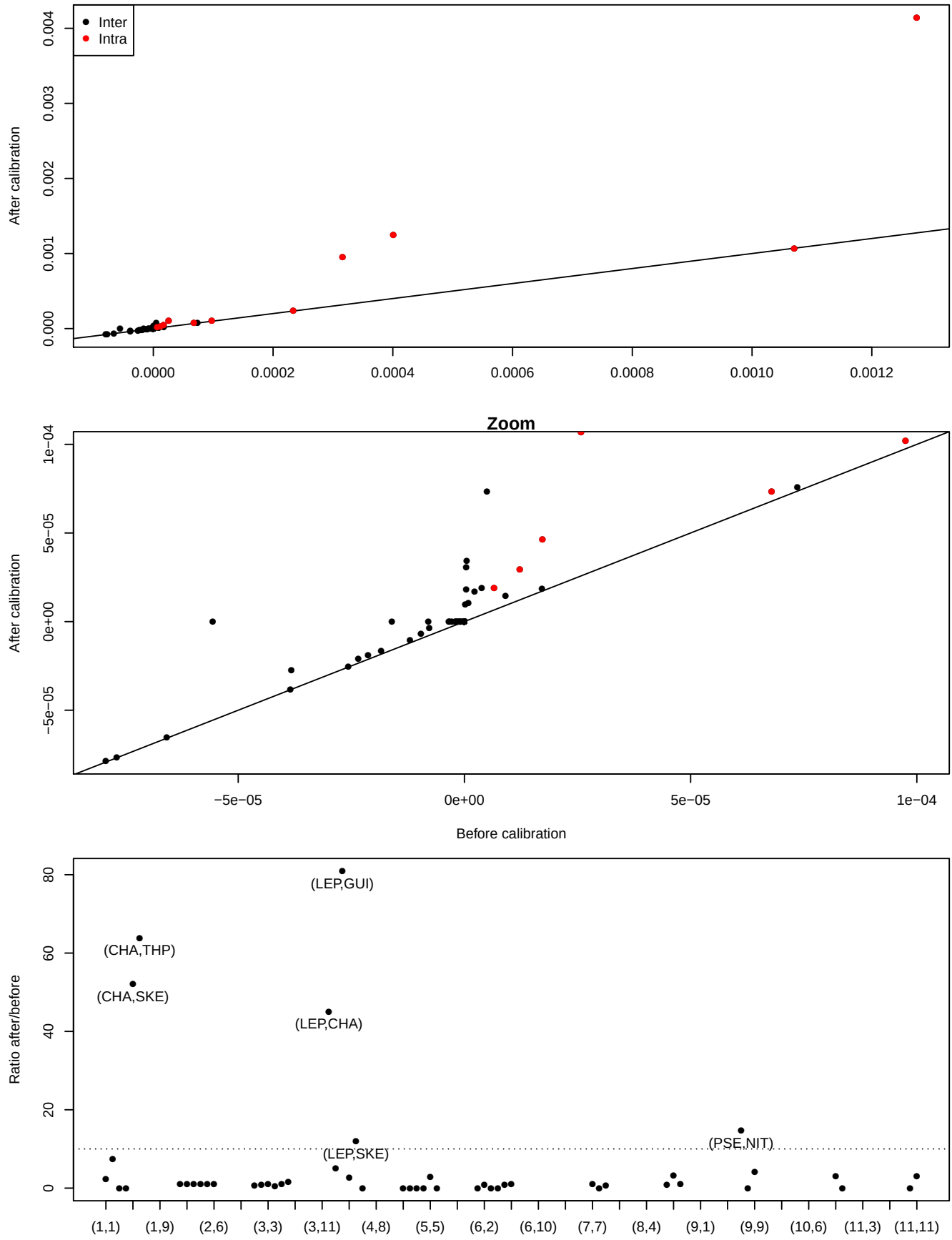

Figure 3: Changes in interaction strengths after calibration by quadratic programming. The middle panel is a zoom on interspecific interaction strengths. Bottom panel shows the ratio of parameter values after and before quadratic programming.

Phytoplankton dynamics

Average abundances seem to be respected but blooms do not appear clearly. The variation in abundances due to seasonality is, for now, underestimated. Species with a lower thermal optima such as Skeletonema miss their two blooms.

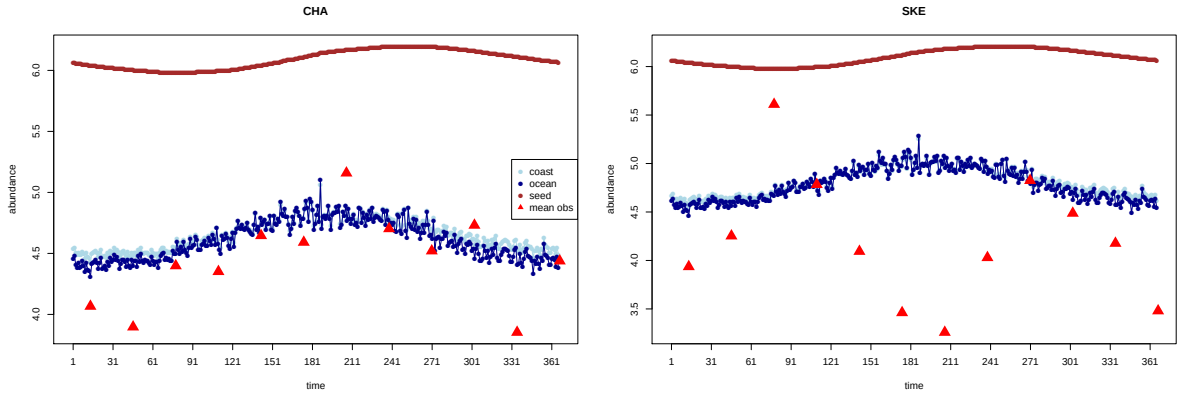

Figure 4: Examples of phytoplankton dynamics (Chaetoceros on the left, Skeletonema on the right)

Thermal optima need to be redesigned in relation to niche area. For now, species with a preference for low temperatures also have a wider niches which buffers their growth. Moreover, a distinction between generalists and specialists species (Hernandez-Farinas et al. 2015). could emerge from the modification of the growth rate formula.

Supplementary Information

Growth rate

Phytoplanktonic growth rates are highly variable, in situ or in experimental conditions. For ten strains in one genus only, and in the same experimental conditions, Balzano *et al.* (2011) have been able to detect growth rates between 0.5 and 1.25 day^{-1}, which corresponds more generally to the values found in the literature (between 0.2 and 1.78 for diatoms, even reaching 3 in the meta-analysis of 308 experiments by Edwards *et al.* (2015); this can be much lower for dinoflagellates). These growth rates are maximum, fixed values for isolated species in laboratory conditions. Most of the time, they correspond to fixed temperature conditions, or to only a small set of values. These observations therefore cannot accomodate realistic, seasonal environment.

In this context, Bissinger *et al.* (2008) based their study on a seminal work by Eppley (1972) to compute the maximum possible growth rate depending on the temperature. The relationship between temperature and growth rate, evaluated on a large database[4], is then $r(T) = 0.81\mathrm{e}^{0.0631T}$,with T in °C. This represents the daily growth rate under a continuous irradiance and can therefore be at least halved because mean daylight is around 12 hours. In this case, growth rates vary between 0.5 and 1.9, in line with previous observations. However, these values only illustrate an exponential growth which cannot be realistic for species which actually show different niche temperatures.

Scranton & Vasseur (2016) designed an equation that distinguised different niches based on optimal temperature.

[4] 1,501 data points from several studies

$$
\begin{aligned}
r_i(T) &= a_r(\tau_0) e^{E_r \frac{(T-\tau_0)}{kT\tau_0}} f_i(T) \\
\text{where } f_i(T) &= \begin{cases} e^{-|T-T_i^{opt}|^3/b_i}, & T \leq T_i^{opt} \\ e^{-5|T-T_i^{opt}|^3/b_i}, & T > T_i^{opt} \end{cases} \\
\text{and} \quad b_i \text{ is defined by numerically solving} & \int r_i(\tau) d\tau = A
\end{aligned} \tag{3}
$$

However, the niches described by this growth function are too narrow, corresponding to values close to 0 for temperatures in which phytoplakton can normally grow. The meta-analysis by Edwards et al. (2016) allows to correct, at least qualitatively the growth rates obtained with Scranton and Vasseur.

By increasing the niche area A in Scranton and Vasseur as well as directly increasing the final growth rate by 0.25, thermal niches seem closer to other values in the literature (Fig. 5).

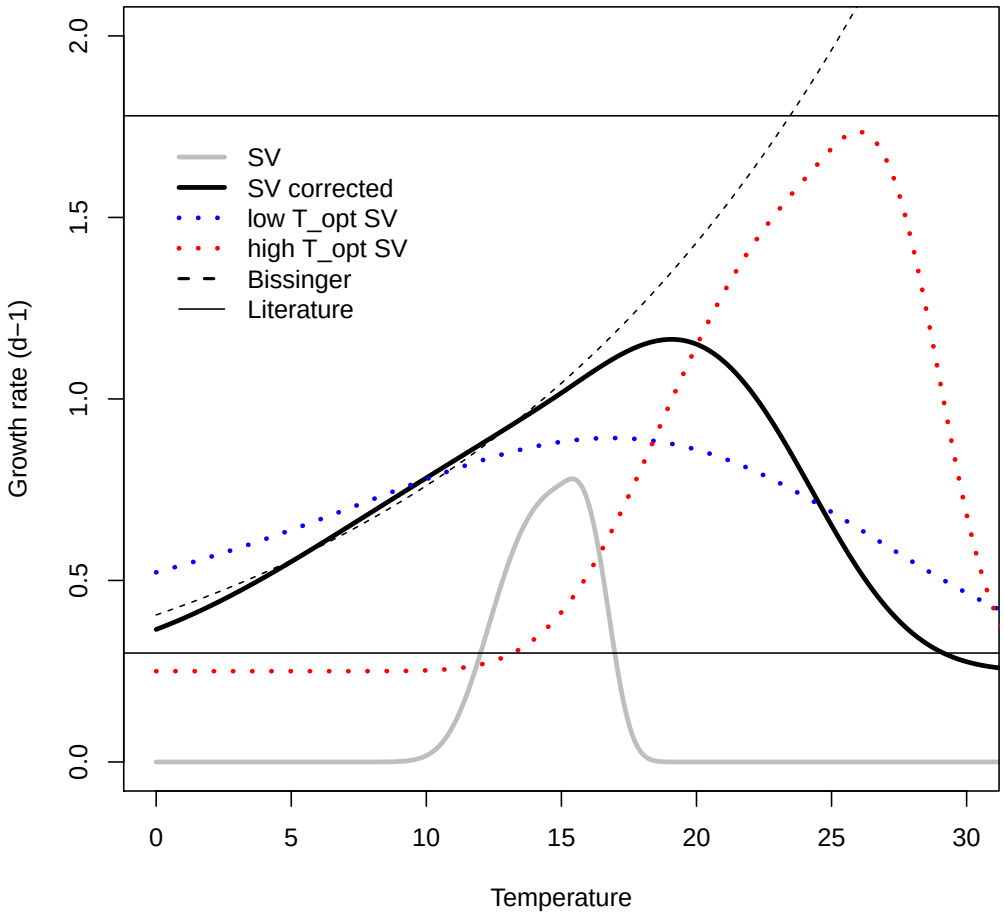

Figure 5: Comparison of growth rate formula

Community matrix: correspondence between Multivariate Autoregressive and Beverton-Holt models

Certain *et al.* (2018)[5] showed that MAR and Beverton-Holt interaction coefficients, respectively b_{ij} and α_{ij}, could map once abundances at equilibrium N_i^* are defined.

$$\begin{cases} b_{ii} - 1 = & \frac{-\alpha_{ii} N_i^*}{1+\sum_l \alpha_{ij} N_l^*} \\ b_{ij,i\neq j} = & \frac{-\alpha_{ij} N_j^*}{1+\sum_l \alpha_{il} N_l^*} \end{cases}$$

Let's define $f_A(i) = \sum_l \alpha_{ij} N_l^*$.

$$b_{ij}(1 + f_A(i)) = -\alpha_{ij} N_j^*$$

We then sum on columns (on j).

$$\sum_j [b_{ij}(1 + f_A(i))] = -f_A(i)$$

$$\Leftrightarrow -f_A(i)(1 + \sum_j b_{ij}) = \sum_j b_{ij}$$

$$\Leftrightarrow f_A(i) = -\frac{\sum_j b_{ij}}{(1 + \sum_j b_{ij})}$$

$$\Leftrightarrow \alpha_{ij} = -\frac{1}{N_j^*} b_{ij} (1 - \frac{\sum_j b_{ij}}{1 + \sum_j b_{ij}})$$

$$\Leftrightarrow \alpha_{ij} = -\frac{1}{N_j^*} \frac{b_{ij}}{1 + \sum_j b_{ij}}$$

This gives an exact correspondance between α_{ij} and b_{ij}.

Quadratic programming

Even though we could directly use the values obtained previously, the switch to another model with a different timestep and the strong uncertainty for all parameters, among other factors of variability, are motivations to calibrate the model more precisely. Maynard *et al.* (2019) have already shown that su an additional calibrations of parameter could lead to more realistic simulations. Followin their example, we use quadratic programming (Bazaraa *et al.*, 2013), applied to interaction matrices and growth rates[6].

The quadratic programming algorithm aims at finding $\mathbf{x}$ that minimizes $||\mathbf{Cx} - \mathbf{d}||^2$ under the constraints $\mathbf{Ex} = \mathbf{f}$ and $\mathbf{Gx} >= \mathbf{h}$.

Here, $\mathbf{C} = \mathbf{I}$, $\mathbf{d} = [\text{vec}(\mathbf{A}^T)^\frown \mathbf{r'}]$ where $\mathbf{A}$ is the interaction matrix, $\mathbf{r'} = -(\mathrm{e}^{\mathbf{r}} - \mathbf{1})$ is the vector of growth rates, $\mathbf{E}$ is built so that we verify the equality $\mathbf{AN}^* + \mathbf{r'} = 0$ where $\mathbf{N}^*$is the vectore of abundance at equilibrium (more precisely, here, average abundance values over the whole time series), and $\mathbf{G}, \mathbf{h}$ so that $\mathbf{r} > 0$ (genera have a positive growth rate when taken in isolation) and $\forall i, a_{ii} > 0$ (negative density-dependence, individuals from the same genus compete with each other).

Mortality in the sediment: McQuoid *et al.* (2002) present maximum and mean depth at which germination of diatoms and dinoflagellates occurred in sediments. They also present sediment datation according to depth. Depth can therefore be related to maximum and mean age of phytoplankton before death.

[5]Corrected in the Appendices of Picoche & Barraquand (2020)

[6]Actually, Maynard et al. 2019 uses a Least Square Inverse Problem solver, with a package (limSolve::lsei) that also offers quadratic programming

Assuming m is the probability of mortality, m follows a geometric law, i.e., m is the probability distribution of the number of days needed for a phytoplankon spore to die. The expectancy for the life duration (the number of days without dying) is $\frac{1}{m} \Leftrightarrow m = \frac{1}{L_{mean}}$where L_{mean} is the average life duration.

Another way to look at the process is that life expectancy L follows the distribution $p(L > l) = e^{-ml}$.With maximum values, we can arbitrarily choose that for these values $p(L > l_{max}) = 0.05$. In this, $m = -\frac{ln(p(L>l_{max}))}{l_{max}}$.

In both cases, $m \propto 10^{-4}\mathrm{d}^{-1}$.

References

Agrawal, S.C. (2009). Factors affecting spore germination in algae - review. *Folia Microbiol*, 54, 273–302.

Balzano, S., Sarno, D. & Kooistra, W.H.C.F. (2011). Effects of salinity on the growth rate and morphology of ten Skeletonema strains. *Journal of Plankton Research*, 33, 937–945.

Bazaraa, M.S., Sherali, H.D. & Shetty, C.M. (2013). *Nonlinear programming: theory and algorithms*. John Wiley & Sons.

Bissinger, J., Montagnes, D., Harples, J. & Atkinson, D. (2008). Predicting marine phytoplankton maximum growth rates from temperature: Improving on the Eppley curve using quantile regression. *Limnology and Oceanography*, 53, 487–493.

Cáceres, C.E. (1997). Temporal variation, dormancy, and coexistence: A field test of the storage effect. *Proceedings of the National Academy of Sciences*, 94, 9171–9175.

Certain, G., Barraquand, F. & GÃ¥ardmark, A. (2018). How do MAR(1) models cope with hidden nonlinearities in ecological dynamics? *Methods in Ecology and Evolution*, 9, 1975–1995.

Edwards, K., Thomas, M., Klausmeier, C. & Litchman, E. (2015). Light and growth in marine phytoplankton: allometric, taxonomic, and environmental variation: Light and growth in marine phytoplankton. *Limnology and Oceanography*, 60, 540–552.

Eilertsen, H., Sandberg, S. & TÃžllefsen, H. (1995). Photoperiodic control of diatom spore growth; a theory to explain the onset of phytoplankton blooms. *Mar. Ecol. Prog. Ser.*, 116, 303–307.

Ellegaard, M. & Ribeiro, S. (2018). The long-term persistence of phytoplankton resting stages in aquatic 'seed banks'. *Biological Reviews*, 93, 166–183.

Eppley, R. (1972). Temperature and phytoplankton growth in the sea. 70.

Fransz, H. & Verhagen, J. (1985). Modelling research on the production cycle of phytoplankton in the Southern Bight of the North Sea in relation to riverborne nutrient loads. *Netherlands Journal of Sea Research*, 19, 241–250.

Kowe, R., Skidmore, R., Whitton, B. & Pinder, A. (1998). Modelling phytoplankton dynamics in the River Swale, an upland river in NE England. *Science of The Total Environment*, 210, 535–546.

Le Pape, O., Jean, F. & Ménesguen, A. (1999). Pelagic and benthic trophic chain coupling in a semi-enclosed coastal system, the Bay of Brest (France):a modelling approach. *Mar. Ecol. Prog. Ser.*, 189, 135–147.

Maynard, D.S., Wootton, J.T., ServÃ¡n, C.A. & Allesina, S. (2019). Reconciling empirical interactions and species coexistence. *Ecology Letters*, 22, 1028–1037.

McQuoid, M.R., Godhe, A. & Nordberg, K. (2002). Viability of phytoplankton resting stages in the sediments of a coastal Swedish fjord. *European Journal Phycology*, 37, 191–201.

Nguyen, V., Buckley, Y.M., Salguero-Gómez, R. & Wardle, G.M. (2019). Consequences of neglecting cryptic life stages from demographic models. *Ecological Modelling*, 408, 108723.

Passow, U. (1991). Species-specific sedimentation and sinking velocities of diatoms. *Mar. Biol.*, 108, 449–455.

Picoche, C. & Barraquand, F. (2019). How self-regulation, the storage effect, and their interaction contribute to coexistence in stochastic and seasonal environments. *Theoretical Ecology*.

Picoche, C. & Barraquand, F. (2020). Strong self-regulation and widespread facilitative interactions between genera of phytoplankton. preprint, bioRxiv.

Plus, M., Dumas, F., Stanisière, J.Y. & Maurer, D. (2009). Hydrodynamic characterization of the Arcachon Bay, using model-derived descriptors. *Continental Shelf Research*, 29, 1008–1013.

Sanyal, A., Larsson, J., van Wirdum, F., Andrén, T., Moros, M., Lönn, M. & Andrén, E. (2018). Not dead yet: Diatom resting spores can survive in naturefor several millennia. preprint, bioRxiv.

Scranton, K. & Vasseur, D.A. (2016). Coexistence and emergent neutrality generate synchrony among competitors in fluctuating environments. *Theoretical Ecology*, 9, 353–363.

Shoemaker, L.G. & Melbourne, B.A. (2016). Linking metacommunity paradigms to spatial coexistence mechanisms. *Ecology*, 97, 2436–2446.

Smayda, T.J. (2002). Turbulence, watermass stratification and harmful algal blooms: an alternative view and frontal zones as "pelagic seed banks". *Harmful Algae*, 1, 95–112.

Wiedmann, I., Reigstad, M., Marquardt, M., Vader, A. & Gabrielsen, T. (2016). Seasonality of vertical flux and sinking particle characteristics in an ice-free high arctic fjord-Different from subarctic fjords? *Journal of Marine Systems*, 154, 192–205.

Wisnoski, N.I., Leibold, M.A. & Lennon, J.T. (2019). Dormancy in metacommunities. *The American Naturalist*, 194, 135–151.